Al-Qadisiyah JournalFor Engineering Sciences 19 (2026) 081 – 086

Contents lists available at: http://qu.edu.iq

Al-Qadisiyah Journal for Engineering Sciences

Journal homepage: https://qjes.qu.edu.iq

Research Paper

Pediatric bone age assessment with AI models based on modified Tanner-Whitehouse

Mohammed Saadi Radeaf [1] ✉, ***Hadeel k. Aljobouri*** [1], ***Noor Kathem AL-Waely*** [1] ***and Oktan Algin*** [2]

[1] *Department of Biomedical Engineering, College of Engineering, Al-Nahrain University, Baghdad, Iraq.*
[2] *National MR Research Center (UMRAM), Bilkent University, 06800 Ankara, Turkey.*

ARTICLE INFO

Article history:
Received 11 August 2024
Received in revised form 10 July 2025
Accepted 18 November 2025

keyword:
BAA
Hand X-ray
GoogleNet
Inception v3
ResNet50
R-CNN
TW3

ABSTRACT

Assessment of bone age, which represents the development and maturity of bones. It helps treat various pediatric conditions and address legal issues. Conventional bone age assessment is a complex and laborious procedure that is susceptible to inconsistencies between different reviewers and within the same reviewer. Artificial intelligence is a new automatic, accurate, and fast method used to evaluate bone age from X-ray images. In this work, a new network design based on AI methods is proposed. This network is based on the dataset obtained from the Paediatric Bone Age Challenge organized by the Radiological Society of North America. The collection comprises 12,600 radiological pictures of left hands, each labeled with the patient's bone age and sex. The design involves two steps: first, using a Faster R-CNN mask by training the ResNet50 model to select regions of interest and then entering the selected regions into three models (Inception v3, GoogleNet, and ResNet50) for regression-based bone age estimation. The results from these models vary based on their internal structure. ResNet50 yields a mean absolute error (MAE) of 10.6 for males and 9.5 for females. Inception v3 has an MAE of 7.5 and 8.3 for Males and females, and GoogleNet has an MAE of 8.4 for males and 9.2 for females. These models can enhance the precision and effectiveness of bone age prediction.

1. Introduction

Bone Age Assessment (BAA) is frequently Stated as a method of evaluating pediatric skeletal age, which is a medical way of evaluating the phase of skeletal growth of a youngster [1]. BAA is not presenting a new field of ability in medical knowledge, was used in the old Roman Kingdom as an Indicator for conscripting adolescent males for military service [2]. BAA is an accurate indicator for the diagnosis of many sicknesses and problems [3]. BAA aims to evaluate development and adulthood and to diagnose and manage pediatric illnesses [4]. Therefore, the accuracy of BAA is crucial. Traditional BAA techniques have been employed for an extended period; nevertheless, the primary issue with these methods is the lack of consistency between different reviewers within the same reviewer [5, 6]. The process of manually assessing bone age normally entails capturing an X-ray image of the left hand and then comparing it to established reference standards. Two methods are proposed, mentioned and used most often in this context: Greulich and Pyle's Handbook of skeletal age determination and Tanner – Whitehouse estimation. Tanner Whitehouse approach is followed by Brian Palmer Sharanakara, confused Granada initiates Palmar [[7, 8]. The bone age is typically estimated using the Greulich and Pyle (non-empirical) atlas which was published by Tanner for the first time in 1959 [9]. Information collected by clinicians for estimating the mature bone age for existing and future practices is termed a reference. The doctor compares the x-ray of the left hand to an image in the atlas based on his or her knowledge and skill [10]. As against the Tanner Whitehouse method, the latter focuses on a detailed measurement of 'Regions of Interest' within the bones of the left hand [11–14]. Instead of relying on visual assessment as in the G&P method, which involves appraising bones within the same hand by sight, the Tanner Whitehouse approach employs that each of the pieces of bone under consideration is given a number score. The TW3 version of this procedure moves a step forward in terms of being comprehensive as it includes more regions such as the ulnar, short bones and radius, Fig. 1. Tanner Whitehouse Method includes the sex differentiation which in many cases it is absolutely necessary when one considers children, as growth patterns can be exceedingly distinctive in girls and boys [15, 16]. Bo Liu et al. [17] also investigated a two stage BAA system in the year 2017. At the first stage, a CNN named VGG-U-Net is employed to segment hand and wrist area from the X-ray image. Then, a conditional Generative adversarial network was built to evaluate bone age. The RSNA2017 Pediatric Bone Age dataset was adopted. The approach yielded an average MAE of bone age estimation of 6.05 months, being 6.01 for males and 6.09 for females at the subgroup level. In 2018, Larson et al. [18] were interested in the problem of estimate the skeletal maturity based on the pediatric hand radiographs using the deep-learning convolutional neural network (CNN). Comparison of the results of the model with the performance of radiologists and automatic models. Showed that for the CNN model MAE was 0.50 years. This improvement could greatly help the diagnosis of the condition in pediatric radiology. In 2018, Vladimir I. Iglovikov et al. [19] described a deep learning technique developed for estimating the bone age of children based on the RSNA2017 Paediatric Bone Age dataset. The method contained not only a complete pre processing sequence but it also included training (CNNs) on segmented and normalized left X-ray images of hand.

* *Corresponding Author.*
E-mail address: Mohammed Saadi@ gmail.com ; Tel: (+964) 771-397 7098 (Mohammed Radeaf)

https://doi.org/10.30772/qjes.2024.152727.1365
2411-7773

Nomenclature

Cp	Specific heat $(J/kg\ K)$	*Greek Symbols*	
k	Thermal conductivity $(W/m\ K)$	α	Thermal diffusivity (m^2/s)
kr	Thermal conductivity ratio, $(kr = kw/kf)$	β	Thermal expansion coefficient $(1/K)$
L	Length of the enclosure (m)	Φ	Solid volume fraction
Lb	Baffle length (m)	Θ	Dimensionless temperature
Nul	Local Nusselt number along with the heat source	ϕ	Baffle inclination angle
Nu	Average Nusselt number	μ	Dynamic viscosity (kg/ms)
p	pressure (kg/ms)	*Subscripts*	
P	Non-dimensional pressure	av	average
Pr	Prandtl number	b	baffle
Ra	Rayleigh number	c	cold
T	Dimensional temperature	f	fluid (pure water)
U	Non-dimensional velocity component X-direction	h	hot
V	Non-dimensional velocity components Y-direction	nf	nanofluid
wb	Baffle width (m)	p	nanoparticle
X	Non-dimensional X-coordinates	s	solid
Y	Non-dimensional Y-coordinates	w	wall

Different hand bone meanings were comprehended by training different models on different regions of hand. the procedure produced a (MAE) of 4. In the year 2019, Eric Wu et al. [20] developed a network based on residual attention, which was designed for hand bones age assessment. Their method used a Mask R-CNN subnet to gate-crash the region of interest in an X-ray picture none the less removing all extraneous components. A residual attention model was designed to perform bone age evaluation in a more clinical environment based on bony areas and achieved a mean absolute error MAE of 7.8. In the year 2021, David K. et al. [21] carried out a study using a prospective multicenter randomized controlled experiment to determine whether artificial intelligence algorithm really improves the accuracy of skeletal age assessment. was made a study allowing radiologists with and without AI in the decision making process using RSNA Paediatric Bone Age dataset. The results indicated that application of the AI algorithm, average skeletal age assessment difference was reduced from 5.95 MAD to 5.36 MAD. In 2021, JIN HE & DAN JIANG [22] proposed a lossless image density based end-to-end BAA model along with a squeeze-and-excitation deep residual network SE ResNet. This method applied to the RSNA 2017 challenge data achieved a MAE of 7.35.

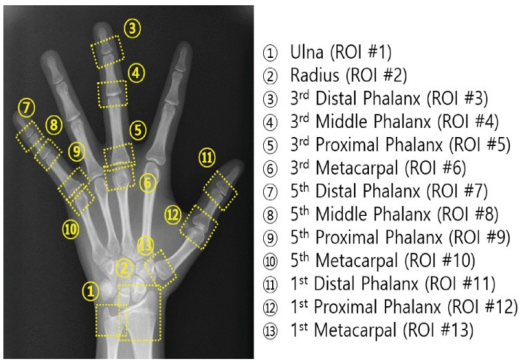

Figure 1**.** ROIs are used in the TW3 metho [23].

In 2021, KEXIN LI et al . [5] evaluated a deep convolutional neural network (CNN) model based on fine-grained image classification, using an image dataset provided by RSNA Experimental outcomes show that the planned method reaches MAE at 7.55 ± 3.71 and 7.74 ± 3.81 months for males and females, respectively. In 2021, Shaowei Li et al. [24] developed A computer-aided diagnosis method utilising deep learning proposed for performing BAA. A proposed image processing pipeline was developed based on a comprehensive unsupervised learning mechanism. The prediction head embedded into the feature vector produced from the backbone model incorporated gender information as an extra input. The analysis revealed a mean absolute inaccuracy of 6.2 months on the RSNA dataset and 5.1 months on the supplementary dataset when MobileNetV3 was employed as the backbone. In 2022, Chi-Chang Chen& Yu-Xian Chou. [10] used four AI models, ResNet50, VGG16, Xception, and ResNet152, to predict the bone ages of X-rays from the RSNA dataset. Xception gets better results than the other models. The MAE was 7.21 months. In 2023, Xiongwei Mao et al.[6] designed a two-stage convolutional transformer network to enhance the precision of BAA. By integrating object recognition and a transformer, the initial phase replicates the bone age analysis procedure performed by paediatricians. It efficiently identifies and extracts the region of interest (ROI) in real-time using YOLOv5. Gender is incorporated into the feature map. The second stage involves the extraction of features specifically inside the region of interest (ROI). The proposed method is assessed using the data from the Paediatric Bone Age Challenge prearranged by RSNA. The experimental results show that the technique achieves (MAE) of 6.22. In the proposed study, the ResNet50 model was used for the detection of the region of interest, and three other models were suggested (Inception v3, GoogleNet, and ResNet50) for the estimation of bone age from X-ray images. The first proposed model utilized ResNet50 for feature extraction from left-hand X-ray images and then ROI selection depending on the training label. The other models used the image crop from the first model as input for the regression of bone age. The major contributions of this research work are:

- Prepressed, Rearranged, and labeled the data set.
- Use deep learning techniques to design an automatic ROI detection depending on the Faster R-CNN mask and the predicted bone age from an X-ray image.

2. Methodology

This section details shown in the pipeline Fig. 2. Starting from the dataset followed by the pre-processing method used to improve the image quality and increase colour contrast. Then, described in detail how to select a region of interest (ROI) and train a special Resnet50 for this purpose. The result from Resnet50 used to train another model to evaluate bone age. The environment used to conduct the study was the following:

- MATLAB 2024A with computer vision
- Windows 11 64bit
- GPU: Nvidia RTX 2070
- RAM: 32 GB

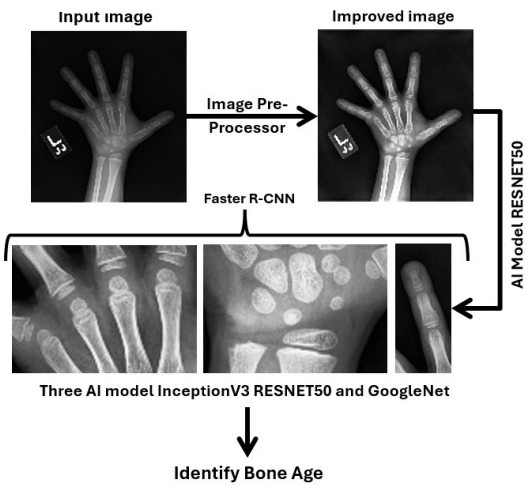

Figure 2**.** Pipeline of BAA.

2.1 Dataset

The proposed methodology was developed using the publicly available RSNA dataset, which comprises 12,611 X-ray images. Figure 3 presents sample images extracted from this dataset. The dataset includes the following attributes:

- ID: An identifier for each photograph.
- Bone age: Bone age for images, represents the truth table.
- Gender: Gender info, indicated as male (true) or female (false).

To improve the quality and contrast of the X-ray image, a multi-step preprocessing procedure was used. This procedure included resizing, rotation, image histogram equalization (imhist), contrast-limited adaptive histogram equalization (CLAHE), and conversion of the grey image to Red, Green & Blue (RGB) format as shown in Fig. 4.

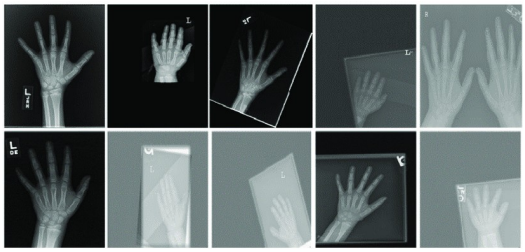

Figure 3. Samples taken from the dataset.

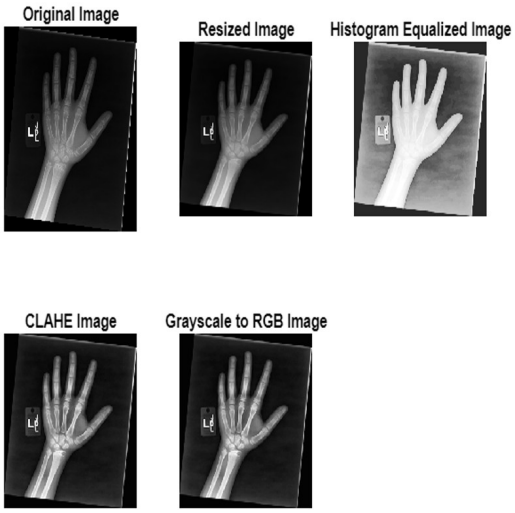

Figure 4. Preprocessor.

2.2 Faster R-CNN Mask

To automatically select an ROI that fits the modified TW3 criteria, as shown in Fig. 5, a modified ResNet50 model was employed along with a region proposal network (RPN). The following steps were used to create a Faster R-CNN mask:

- Resize images to 299×299 to provide more acceptable data for the neural network.
- Preprocess the images using (CLAHE).
- Manually annotate the ROI for 294 random images and select three boxes, as shown in Fig. 3, using an image labeler.
- Divide the dataset into 60% for training, 10% for validation, and 30% for testing.
- Use augmented data to improve network accuracy.
- Modify the ResNet50 model by removing the last three layers (fc1000, c1000-softmax, ClassificationLayer-fc1000).
- Define new classification layers (rcnnFC, rcnnSoftmax, rcnnClassification).
- Add an ROI max pooling layer and connect it to the feature extraction layer activation-40-relu as in Fig. 6.

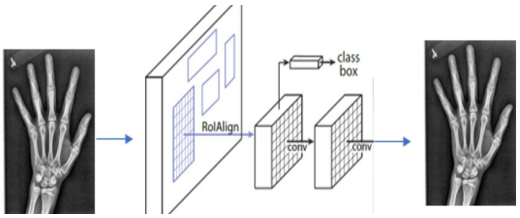

Figure 5. Region selection based on modified TW3.

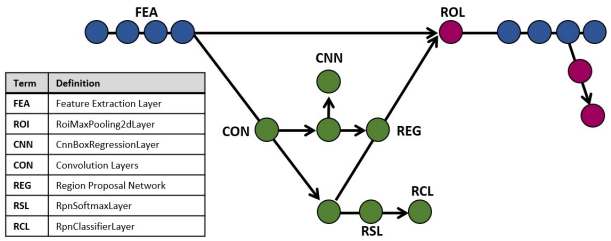

Term	Definition
FEA	Feature Extraction Layer
ROI	RoiMaxPooling2dLayer
CNN	CnnBoxRegressionLayer
CON	Convolution Layers
REG	Region Proposal Network
RSL	RpnSoftmaxLayer
RCL	RpnClassifierLayer

Figure 6. Faster R-CNN layers.

2.3 Regression

The BAA model presented in this paper is a convolutional neural network: Inception v3, ResNet50, and GoogLeNet. To modify these models to do regression, specific modifications were made to each architecture. Improvement of the model's result, the data was combined with age as inputs. By Merage both image and age, the profit from additional background information leads to improved performance in bone age prediction.

2.3.1 Inception v3

Inception v3 is a convolutional neural network intended to aid with picture analysis and object detection. It is the third iteration of Google's Inception model. The convolutional neural network used several novel techniques, including the RMSProp optimizer, factorized 7×7 convolutions, BatchNorm in the auxiliary classifiers, and smoothing labeling. Factorizing convolutions reduces the parameter count while maintaining network efficiency [25]. To the regression model, the last three layers ('predictions', 'predictions-softmax,' and 'ClassificationLayer-predictions') were removed. In their place, regression layers were added, specifically a fully connected layer and a regression layer, as illustrated in Fig. 7. This modification enables the network to predict continuous values, such as bone age, rather than categorical outputs.

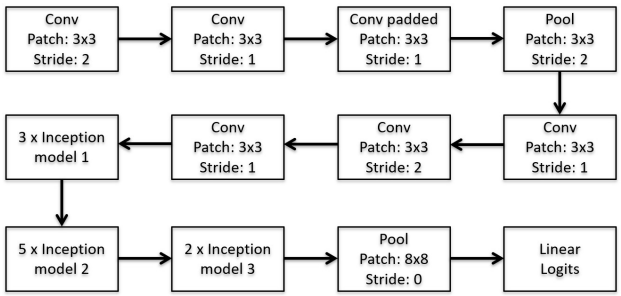

Figure 7. Inception v3 internal layer [26].

2.3.2 ResNet50

The ResNet50 is a convolutional neural network renowned for its exceptional performance in picture classification. ResNet implemented residual networks as an intermediary between layers, resulting in a reduction in loss, retention of acquired knowledge, and enhanced performance throughout the training phase [27, 28]. A block diagram of the ResNet model's architecture is shown in Fig. 8. Similarly, the ResNet50 model was adapted by removing its final layers ('fc1000', 'fc1000-softmax', 'ClassificationLayer-fc1000') and adding regression-specific layers to calculate bone age.

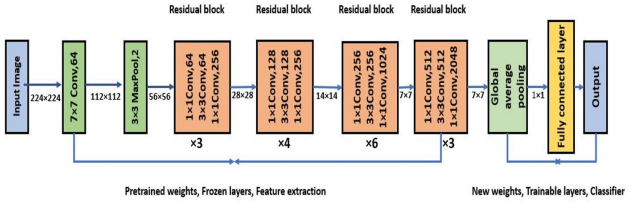

Figure 8. The architecture of the ResNet-50 model.

2.3.3 GoogLeNet

GoogLeNet is a specific convolutional neural network that was developed based on the Inception design. The network employs Inception modules, which enable the selection of several convolutional filter sizes inside each block. GoogLeNet specifically denotes the specific version of the Inception architecture. The system employed a more extensive and widely implemented Inception network that exhibited a somewhat higher level of quality [29]. A block diagram of the GoogLeNet architecture is shown in Fig. 9. GoogLeNet was also modified to include regression layers after removing the final classification layers ('loss3-classifier', 'prob', 'output'). The change enables the AI model to output number values.

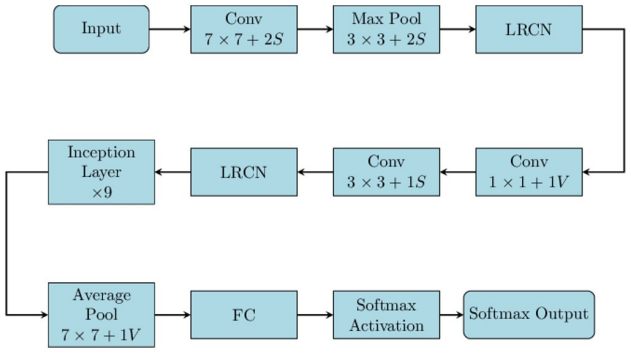

Figure 9. The architecture of GoogLeNet [30].

3. Results and discussion

3.1 Dataset

The dataset of 12,611 X-ray images was divided into three subsets for the development and evaluation of the model:

- Training: 70% (8,827 images).
- Validation: 15% (1,892 images).
- Test: 15% (1,892 images).

3.2 Faster R-CNN Mask

The results of training the model presented by the precision-recall (PR) curve of the ResNet50 model, which achieved an average precision of 0.79, as shown in Fig. 10. The test results of the ResNet50 model are presented in Table 1. The scoring system was constrained by a specific threshold code (≥ 0.85). Only results that accurately exceed 85% are included in the final output, as illustrated in Fig. 11. During training, the detector was employed to crop all image inputs to focus on specific regions of interest. This targeted approach ensures that the regression model concentrates on the most relevant areas, thereby enhancing the accuracy and efficiency of bone age prediction.

Table 1. Results of Testing Resnet 50.

#	Boxes	Scores	Labels
1	5 × 4	[0.9830;0.9903;0.9924;0.9697;0.7655]	5 × 1
2	5×4	[0.9955;0.9984;0.5610;0.7814;0.9747]	5 × 1
3	5×4	[0.9965;0.9916;0.8712;0.9958;0.6978]	5 × 1
4	4×4	[0.9860;0.9952;0.9965;0.8905]	4 × 1
5	7×4	[0.9905;0.9956;0.9220;0.7169;0.9850;0.8534;0.9534]	7 × 1
6	5×4	[0.9940;0.9839;0.9916;0.5743;0.6041]	5 × 1
7	4×4	[0.9882;0.9926;0.9982;0.9595]	4 × 1
8	4×4	[0.9898;0.9923;0.8734;0.8027]	4 × 1
9	3×4	[0.9804;0.9981;0.9967]	3 × 1
10	4×4	[0.9857;0.9964;0.9983;0.8784]	4 × 1
11	4×4	[0.9936;0.9744;0.5633;0.9969]	4 × 1
12	6×4	[0.9844;0.9960;0.9955;0.8469;0.9252;0.6196]	6 × 1
13	6×4	[0.8895;0.9985;0.7321;0.9957;0.9174;0.8798]	6 × 1
14	5×4	[0.9921;0.9688;0.7902;0.6406;0.9877]	5 × 1

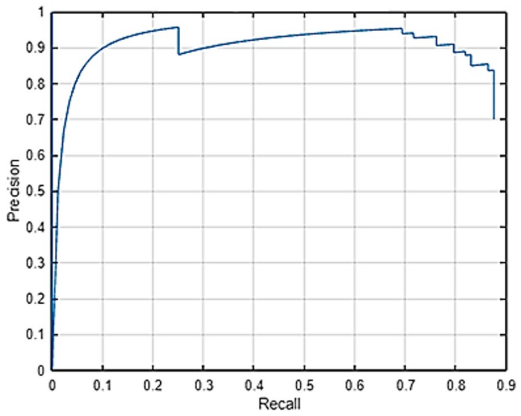

Figure 10. Precision-Recall (PR) curve.

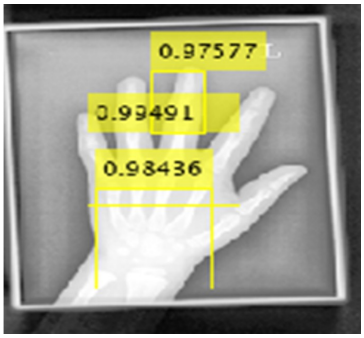

Figure 11. Result of Faster R-CNN mask.

3.3 Regression

The proposed models were implemented to extract features and regression bone age from X-ray images. To execute these models, the software installed on the Windows computer included MATLAB with computer vision and image labeler package. The training of the Models (ResNet50, Inception v3, and GoogLeNet) models for the males' dataset and females using a special option was as follows:

- Solver name: SGDM
- Learning rate:1e-6
- MaxEpochs: 32
- Shuffle: every epoch
- Validation Frequency: 30
- Verbose: True

The results of the training are shown in Table 2.

These results indicate the use of the inception v3 model achieved lower MAEs 7.5 and 8.3 for males and females respectively. This proves the ability of Inception v3 to effectively learn essential features, as it assigns higher weights to those features that contribute significantly to the model's performance improvement. In contrast, the ResNet50 gives a higher MAE comparison with the other two models.

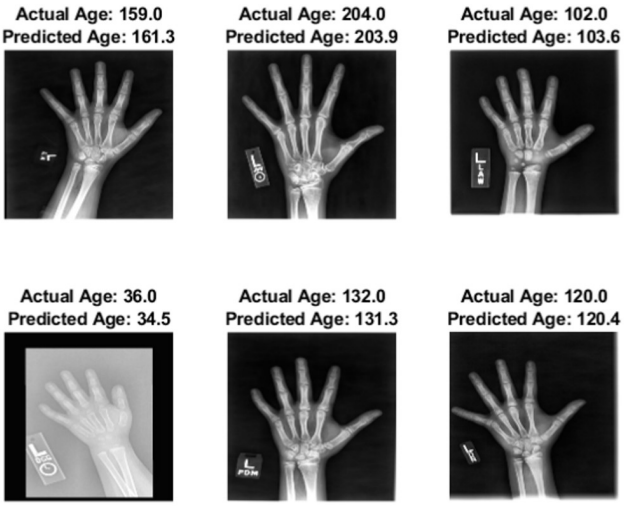

Figure 12**.** Actual and predicted age using Inception V3.

This study proposed a technique for solving the problem of BAA by using AI models. Three models (ResNet50, Inception v3, and GoogLeNet) were used to extract features from the crop X-ray image of the left hand by Faster R-CNN mask, Fig. 12. Good performance (7.21 MAE) was achieved on the data preprocessed in the study in 20.3 by Chi-Chang Chen and Yu-Xian Chou [21] when using ResNet50, VGG16, Xception, and ResNet152, to automatically predict the bone ages. In 2023, Xiongwei Mao et al. [6] introduced a two-stage convolutional transformer network to expand the accuracy of BAA and achieved MAE 6.22. This paper proposed Three different models to predict bone age. Inception V3 model achieved lower MAE when compared with ResNet50 and GoogLeNet. Table 3 shows previous methods used to predict bone age compared to the proposed work.

Table 2**.** Results of training.

#	Model	Gender	MAE
1	INCEPTION V3	MALE	(7.5 ± 1.8)
1	INCEPTION V3	FEMALE	(8.3 ± 2.3)
2	ResNet50	MALE	(10.6 ± 0.8)
2	ResNet50	FEMALE	(9.5 ± 0.5)
3	GoogLeNet	MALE	(8.4 ± 0.5)
3	GoogLeNet	FEMALE	(9.2 ± 0.9)

Table 3**.** Comparison of the proposed methods with the literature.

#	Ref.	Methodology	Dataset	MAE
1	[10]	Vgg16, ResNet50, ResNet152, and Xception	RSNA	VGG: 12.47 & 9.95 ResNet50:26.49 &21.17 ResNet152:12.28 &9.81 Xception: 7.21 & 7.21
2	[6]	Vgg16, ResNet50, ResNet152, and Xception	RSNA	Swin transformer: 6.22
3	Proposed method	R-CNN mask with inception V3, ResNet50 & GoogLeNet	RSNA	Inception V3 (7.5 ± 1.8) & (8.3 ± 2.3) ResNet50 (10.6 ± 0.8) & (9.5 ± 0.5) GoogLeNet (8.4 ± 0.5) & (9.2 ± 0.9)

4. Conclusions

This study explores building an Artificial intelligence model for Bone age assessment. Derived from the clinical workflow TW3 of BAA a network based on the RSNA dataset for age assessment. This model consists of two subnets: the R-CNN mask subnet segments hands to different ROI and removes the unwanted background based on anatomical parts mentioned in TW3. Furthermore, three regression models were used to predict age based on gender. This network can be an effective solution for the radiography department, especially in our country, Iraq, which has limited access to medical research and diagnostic options. This model was devised to assist radiologists in detecting the accurate age of pediatric cases. The result can be improved in future work by increasing the number of training images, using image capture by digital X-ray to improve the quality of images, and designing a user interface for easier use.

Authors' contribution

All authors contributed equally to the preparation of this article.

Declaration of competing interest

The authors declare no conflicts of interest.

Funding source

This study didn't receive any specific funds.

Data availability

The data that support the findings of this study are available from the corresponding author upon reasonable request.

REFERENCES

[1] M. Mansourvar, A. Ismail, T. Herawan, R. G. Raj, S. A. Kareem, and F. H. Nasaruddin, "Automated bone age assessment: Motivation, taxonomies, and challenges," *Hindawi Limited, Computational and Mathematical Methods in Medicine*, vol. 2013, no. 1, p. 391626, 2013. [Online]. Available: https://doi.org/10.1155/2013/391626

[2] A. Schmeling, G. Geserick, W. Reisinger, and A. Olze, "Age estimation," *Forensic Sci Int*, vol. 165, no. 2–3, p. 178–181, 2007. [Online]. Available: https://doi.org/10.1016/J.FORSCIINT.2006.05.016

[3] M. Satoh, "Bone age: assessment methods and clinical applications," *J. Clin Pediatr Endocrinol*, vol. 24, no. 4, pp. 143–152, 2015. [Online]. Available: https://doi.org/10.1297/cpe.24.143

[4] M. P. Piotrkowska, K. Marszałek-Dziuba, E. Moszczyńska, M. Szalecki, and E. Jurkiewicz, "Traditional and new methods of bone age assessment-an overview," *J Clin Res Pediatr Endocrinol*, vol. 13, no. 3, pp. 251–262, 2021. [Online]. Available: https://doi.org/10.4274/jcrpe.galenos.2020.2020.0091

[5] K. Li, J. Zhang, Y. Sun, X. Huang, C. Sun, and Q. Xie, "Automatic bone age assessment of adolescents based on weakly supervised deep convolutional neural networks," *IEEE Access*, vol. 9, p. 120078–120087, 2021. [Online]. Available: https://doi.org/10.1109/ACCESS.2021.3108219

[6] X. Mao, Q. Hui, S. Zhu, W. Du, C. Qiu, X. Ouyang, and D. Kong, "Automated skeletal bone age assessment with two-stage convolutional transformer network based on x-ray images," *Diagnostics*, vol. 13, no. 11, p. 1837, 2023. [Online]. Available: https://doi.org/10.3390/diagnostics13111837

[7] N. Poojary, G. Pokhare, P. Poojary, D. Raghavani, and J. Khanapuri, "A novel approach for bone age assessment using deep learning," *International Journal of Scientific Research in Computer Science Engineering and Information Technology*, vol. 7, no. 3, 2021. [Online]. Available: https://doi.org/10.32628/cseit21731

[8] I. S. for Olfaction, I. S. C. Chemical Sensing, I. of Electrical, and E. Engineers, "Isoen 2019: 18th international symposium on olfaction and electronic nose: 2019 symposium proceedings: Acros fukuoka, may 26-29, 2019." *IEEE, Piscataway, NJ*, 2019.

[9] W. Greulich and S. Pyle, "Radiographic atlas of skeletal development of the hand and wrist professor of anatomy, stanford university school of medicine,," 2006.

[10] C. Chen and Y. Chou, "Bone age prediction with AI Models," *International Journal of Computer Trends and Technology*, vol. 71, no. 2, p. 19–24, 2022. [Online]. Available: https://doi.org/10.14445/22312803/ijctt-v71i2p104

[11] M. Vignolo, S. Milani, G. Cerbello, P. Coroli, E. D. Battista, and G. Aicardi, "Fels, greulich-pyle, and tanner-whitehouse bone age assessments in a group of italian children and adolescents," *American Journal of Human Biology*, vol. 4, no. 4, p. 493–500, 1992. [Online]. Available: https://doi.org/10.1002/AJHB.1310040408

[12] B. Lee and M. Lee, "Automated bone age assessment using artificial intelligence: The future of bone age assessment," *Korean J Radiol*, vol. 22, no. 5, pp. 792–800, 2021. [Online]. Available: https://doi.org/10.3348/kjr.2020.0941

[13] C. Yang, W. Dai, B. Qin, X. He, and W. Zhao, "A real-time automated bone age assessment system based on the RUS-CHN method," *Front Endocrinol (Lausanne)*, vol. 14, p. 1073219, 2023. [Online]. Available: https://doi.org/10.3389/fendo.2023.1073219

[14] N. Khalaf, K. Aljobouri, S. Najim, and I. Çankaya, "Simplified convolutional neural network model for automatic classification of retinal diseases from optical coherence tomography images," *Al-Nahrain Journal for Engineering Sciences*, vol. 26, no. 4, p. 314–319, 2024. [Online]. Available: https://doi.org/10.29194/njes.26040314

[15] M. Umer, A. Eshmawi, K. Alnowaiser, A. Mohamed, H. Alrashidi, and I. Ashraf, "Skeletal age evaluation using hand x-rays to determine growth problems," *PeerJ Comput Sci*, vol. 9, p. e1512, 2023. [Online]. Available: https://doi.org/10.7717/peerj-cs.1512

[16] F. Cavallo, A. Mohn, F. Chiarelli, and C. Giannini, "Evaluation of bone age in children: A mini-review," *Frontiers Media S.A.*, vol. 9, 2021. [Online]. Available: https://doi.org/10.3389/fped.2021.580314

[17] B. Liu, Y. Zhang, M. Chu, X. Bai, and F. Zhou, "Bone age assessment based on rank-monotonicity enhanced ranking CNN," *IEEE Access*, vol. 7, p. 120976–120983, 2019. [Online]. Available: http://doi.org/10.1109/ACCESS.2019.2937341

[18] D. Larson, M. Chen, P. Lungren, S. Halabi, V. Stence, and P. Langlotz, "Performance of a deep-learning neural network model in assessing skeletal maturity on pediatric hand radiographs," *Radiology*, vol. 287, no. 1, p. 313–322, 2018. [Online]. Available: https://doi.org/10.1148/radiol.2017170236

[19] V. Iglovikov, A. Rakhlin, A. Kalinin, and A. Shvets, "Paediatric bone age assessment using deep convolutional neural networks," *in Lecture Notes in Computer Science (including subseries Lecture Notes in Artificial Intelligence and Lecture Notes in Bioinformatics), Springer Verlag*, vol. 11045, p. 300–308, 2018. [Online]. Available: https://doi.org/10.1007/978-3-030-00889-5_34

[20] E. Wu, B. Kong, X. Wang, J. Bai, Y. Lu, F. Gao, S. Zhang, K. Cao, Q.Song, S. Lyu, and Y. Yin, "Residual attention-based network for hand bone age assessment," *Computer Vision and Pattern Recognition*, 2019. [Online]. Available: https://doi.org/10.48550/arXiv.1901.05876

[21] D. K. Eng and et al., "Artificial intelligence algorithm improves radiologist performance in skeletal age assessment: A prospective multicenter randomized controlled trial," *Radiology*, vol. 301, no. 3, p. 692–699, 2021. [Online]. Available: https://doi.org/10.1148/radiol.2021204021

[22] J. He and D. Jiang, "Fully automatic model based on se-resnet for bone age assessment," *IEEE Access*, vol. 9, p. 62460–62466, 2021. [Online]. Available: https://doi.org/10.1109/ACCESS.2021.3074713

[23] S. Son, Y. Song, and et al, "TW3-Based fully automated bone age assessment system using deep neural networks," *IEEE Access*, vol. 7, p. 33346–33358, 2019. [Online]. Available: https://doi.org/10.1109/ACCESS.2019.2903131

[24] S. Li, B. Liu, S. Li, X. Zhu, Y. Yan, and D. Zhang, "A deep learning-based computer-aided diagnosis method of x-ray images for bone age assessment," *Complex and Intelligent Systems*, vol. 8, p. 1929–1939, 2022. [Online]. Available: https://doi.org/10.1007/s40747-021-00376-z

[25] A. Linkon, M. Labib, T. Hasan, M. Hossain, and M. Jannat, "Deep learning in prostate cancer diagnosis and gleason grading in histopathology images: An extensive study," *Informatics Med. Unlocked*, vol. 24, no. 3, p. 100582, 2021. [Online]. Available: https://doi.org/10.1016/J.IMU.2021.100582

[26] A. BRITAL, "Inception V3 CNN architecture explained," *Medium*, 2024. [Online]. Available: https://medium.com/@AnasBrital98/inception-v3-cnn-architecture-explained-691cfb7bba08

[27] W. Li, S. Yu, R. Yang, Y. Tian, and et al., "Machine learning model of ResNet50-Ensemble voting for malignant–benign small pulmonary nodule classification on computed tomography images," *Cancers (Basel)*, vol. 15, no. 22, p. 5417, 2023. [Online]. Available: https://doi.org/10.3390/cancers15225417

[28] L. Ali, F. Alnajjar, H. A. Jassmi, M. Gochoo, W. Khan, and M. A. Serhani, "Performance evaluation of deep CNN-based crack detection and localization techniques for concrete structures," *Sensors*, vol. 21, no. 5, p. 1688, 2021. [Online]. Available: https://doi.org/10.3390/s21051688

[29] "GoogLeNet CNN architecture explained (Inception V1)," 2024.

[30] C. Szegedy and et al., "Going deeper with convolutions," *Computer Vision and Pattern Recognition*, p. 4842, 2014. [Online]. Available: https://doi.org/10.48550/arXiv.1409.4842

How to cite this article:
Mohammed Saadi Radeaf, Hadeel k. Aljobouri, Noor Kathem AL-Waely and Oktan Algin (2026). 'Theoretical model to predict the flexural response of concrete beams pre-tensioned with CFRP rods considering CFRP slippage effects', Al-Qadisiyah Journal for Engineering Sciences, 19(1), pp. 081- 086.
https://doi.org/10.30772/qjes.2024.152727.1365